Supporting Information

Novel dinuclear open paddle-wheel-like copper complexes involving π-stacking on the basis of chiral binaphthyl phosphoric acid {(R)-PhosH}: structural, magnetic and optical properties

Humberto A. Rodríguez,[a] Daniel A. Cruz,[a] Víctor Lavín [,b] Juan I. Padrón,[a] and Pablo Lorenzo-Luis[*c]

[a.]Instituto de Productos Naturales y Agrobiología, Consejo Superior de Investigaciones Científicas (IPNA-CSIC), 38206, La Laguna, Tenerife, Islas Canarias: Email: jipadron@ipna.csic.es.

[b.] a.Departamento de Física, MALTA-Consolider Team, and IUdEA, Universidad de La Laguna, Apartado de Correos 456, San Cristóbal de La Laguna, Santa Cruz de Tenerife E-38200, Spain. Email: vlavin@ull.es.

[c] Área de Química Inorgánica, Departamento de Química, Universidad de La Laguna, C/ Astrofísico Francisco Sánchez 3, 38071 La Laguna, Spain. Email: plorenzo@ull.es

Table of contents

1. Material and general procedure.

All reagents were obtained from commercial sources (Apollo®, Merck®, Thermo Fisher Scientific® and BLDpharm®) and used without any further purification. Solvents were dried and distilled before use (except for acetone). The reagents used have been obtained from the following commercial sources, indicating the purity of each of them. The following reagents were purchased from the commercial company Apolllo®: (R)-(-)-1,1'-Binaphthyl-2,2'-diyl hydrogenphosphate 98% (CAS No. 39648-67-4), copper(II) trifluoromethanesulphonate 98% (CAS No. 34946-82-2), zinc(II) trifluoromethanesulphonate 98% (CAS No. 54010-75-2), nickel(II) trifluoromethanesulphonate 100% (CAS No. 60871-84-3). Another were purchased from the commercial company Merck®: iron(II) trifluoromethanesulfonate 85% (CAS No. 59163-91-6), iron(III) trifluoromethanesulfonate 90% (CAS No. 63295-48-7), sodium hydride 60 % dispersion in mineral oil (CAS No. 7646-69-7) and copper(II) phosphate 98% (CAS No. 7798-23-4).

Optical rotation was measured on an Anton Paar- M150 Polarimeter. HRESMS data was performed on a Waters SYNAPT XS ion mobility Q-TOF mass spectrometer by addition of methanol. The centrifugation processes were carried out with the centrifuge VWR Mega Star 3.0R.

1.1. Synthesis procedure of the complex $1 \cdot (C_3H_6O)_2$.

To a 0.05 M suspension of {(R)PhosH} (562.7 μmol) in dioxane, NaH (562.7 μmol) is added, and it is left under vigorous stirring for 1 hour under nitrogen and at room temperature. At the same time, Cu(OTf)$_2$ (562.7 μmol) is dissolved in dioxane (0.05 M), under nitrogen and at room temperature. Then the metal solution is slowly added to that of the ligand, observing a change in hue (from blue to cyan). After vigorous overnight stirring under nitrogen the formation of a white precipitate was observed and eliminated by centrifugation (4000 rpm, 4 min). The solution was allowed to dry completely in air, observing the formation of a silver-blue precipitate. This was dissolved in dichloromethane and the same amount of wet acetone, allowing it to crystallize at low temperature (4-8°C). The resulting cyan-yellow crystals were separated from the solution and analyzed by X-ray structure determination. From a practical standpoint note that by careful soft vacuum process of the crystalline sample $1 \cdot (C_3H_6O)_2$ we obtained a completely anhydrous phase (hereafter **1**), which remained stable under normal conditions of temperature and humidity. 79 % yield (182.0 mg, 55.8 μmol). Melting point: decomposes at 260.3°C. $[\alpha]_D^{25}$: -415.6 (c = 0.99, DMSO).

1.2. Scope of metals of the first transition series.

The scope of the methodology has been carried out for other metals from their respective triflic salts, summarized in **Table 1S**. The synthesis conditions have been the same as those described for complex **1** $(C_3H_6O)_2$.

Table 1S. Scope of complex formation with triflic metal salts and L = {(*R*)PhosH}

(*R*)-(-)-PhosH

Entry	L	$M^{n+}(OTf)^-_n$ (equiv)	Solvent (M)	T(°C)	Atm.	t(h)[a]	Colour	Yield (%)[b][c]
1	1.0	Cu(OTf)$_2$ 1.0	Dioxane 0.0125	RT	N$_2$	o.n.	Cyan-yellov	79%
2	1.0	Fe(OTf)$_2$ 1.0	Dioxane 0.0125	RT	N$_2$	o.n.	Orange	NC
3	1.0	Ni(OTf)$_2$ 1.0	Dioxane 0.0125	RT	N$_2$	o.n.	Pale yellow	NC
4	1.0	Zn(OTf)$_2$ 1.0	Dioxane 0.0125	RT	N$_2$	o.n.	Colorless	NC
5	1.0	Fe(OTf)$_3$ 1.0	Dioxane 0.0125	RT	N$_2$	o.n.	Pale orange	NC
6	1.0	Sc(OTf)$_3$ 1.0	Dioxane 0.0125	RT	N$_2$	o.n.	Colorless	NC

1.3. Infrared analysis for complex 1.

Transmittance measurements were conducted using an ATR PRO ONE spectrometer equipped with a TGS detector, employing an accumulation of 64 scans and a resolution of 8 cm^{-1}. The aperture size was set to 7.1 mm, with a scanning speed of 2 mm/sec and a filter frequency of 10000 Hz.

[a] o.n. = over
[b] Yield of is
[c] NC = not c

Fig. 1S. Comparative IR spectrum of Transmittance (%) for **1** and Cu$_3$(PO$_4$)$_2$ compound.
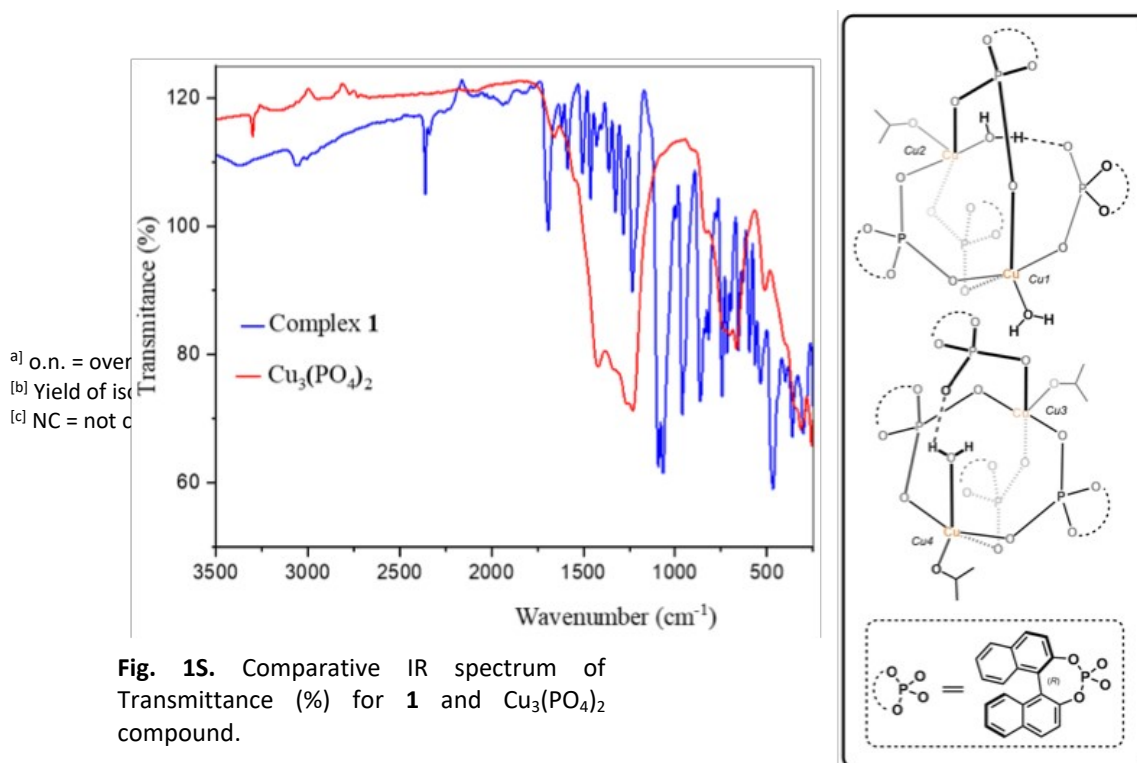
Selection FT–IR data (cm^{-1}) vibrations:[1-3]

3370, 3058 vbr $\nu s/\nu(H_2O)$

1617: $\delta(H_2O)$

3006: $\nu(C\text{-}H)_{arom}$

817, 836, 862: $\pi(C\text{-}H)_{arom}$

1137: -P=O

946: $\nu(M\text{-}O\text{-}P)_{asym}$

1214: $\nu(M\text{-}O\text{-}P)_{sym}$

2339: could be assignable to the $\nu(OH)$ of the P-OH moiety due deprotonation of P–OH groups of the PO_4^{3-} ligand.

References:

1   T. Prapakaran, C. I. Sathish, J. Yi, A. Vinu, and R. Murugavel, *Eur. J. Inorg. Chem.,* 2023, **26**, e202300071.

2   J. C. Belmont-Sánchez, M. E. García-Rubiño, A. Frontera, J. M. González-Pérez, A. Castiñeiras and J. Niclós-Gutiérrez, *Crystals*, 2021, **11**, 48 – 62.

3   T. Harada, Y. Hasegawa, Y. Nakano, M. Fujiki, M. Naito, T. Wada, Y. Inoue and T. Kawai, *Journal of Alloys and Compounds,* 2009, **488**, 599–602.

1.4. NMR analysis for complex 1.

A nuclear magnetic resonance study has been carried out to study the chemical shifts of the organic components of the Cu-Complex. The ^{1}H-NMR and ^{13}C-NMR performed on DMSO-d_6 shows the characteristic aromatic signals of binolic groups, acetone and water. Chemical shifts of phosphorus atoms in **1** could not be detected.

¹H NMR (DMSO-d₆, 500 MHz)

Aromatic signals

H₂O

ketone
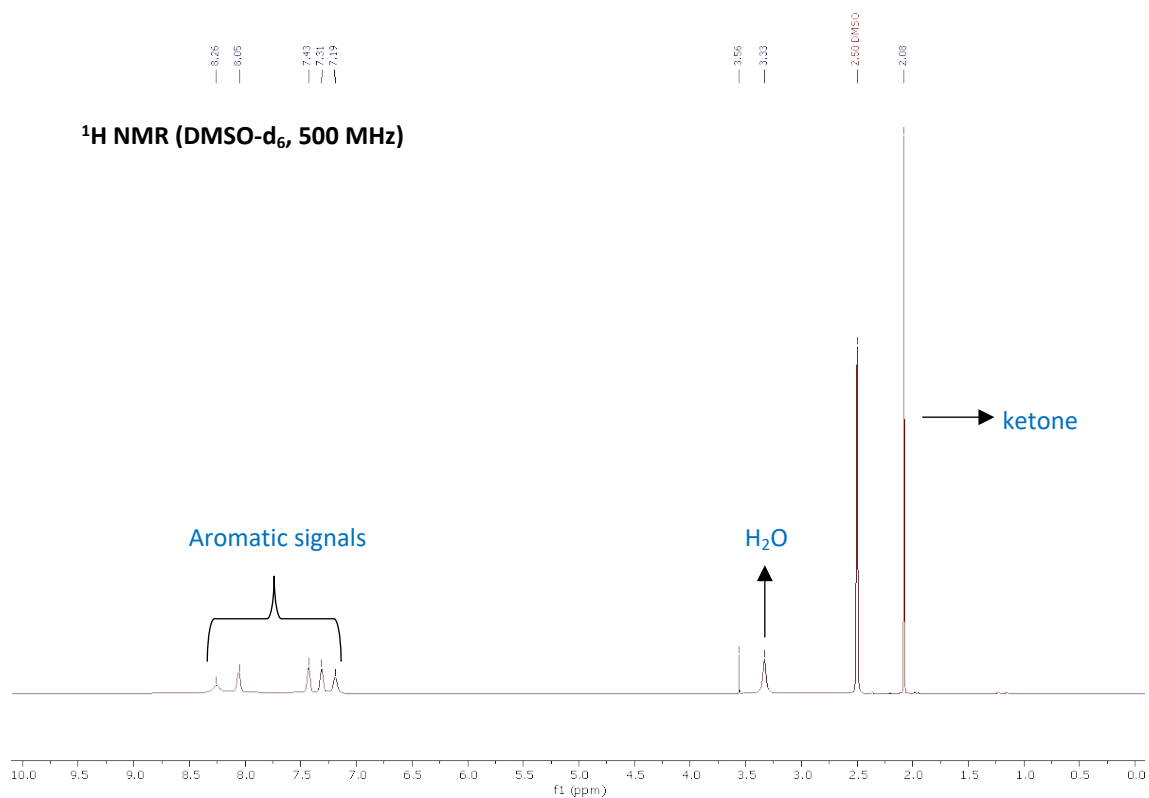
Fig. 2S-a. ¹H- NMR 500 MHz spectra of **1** in DMSO-d₆.

¹³C NMR (DMSO-d₆, 125 MHz)

Aromatic signals

ketone

ketone
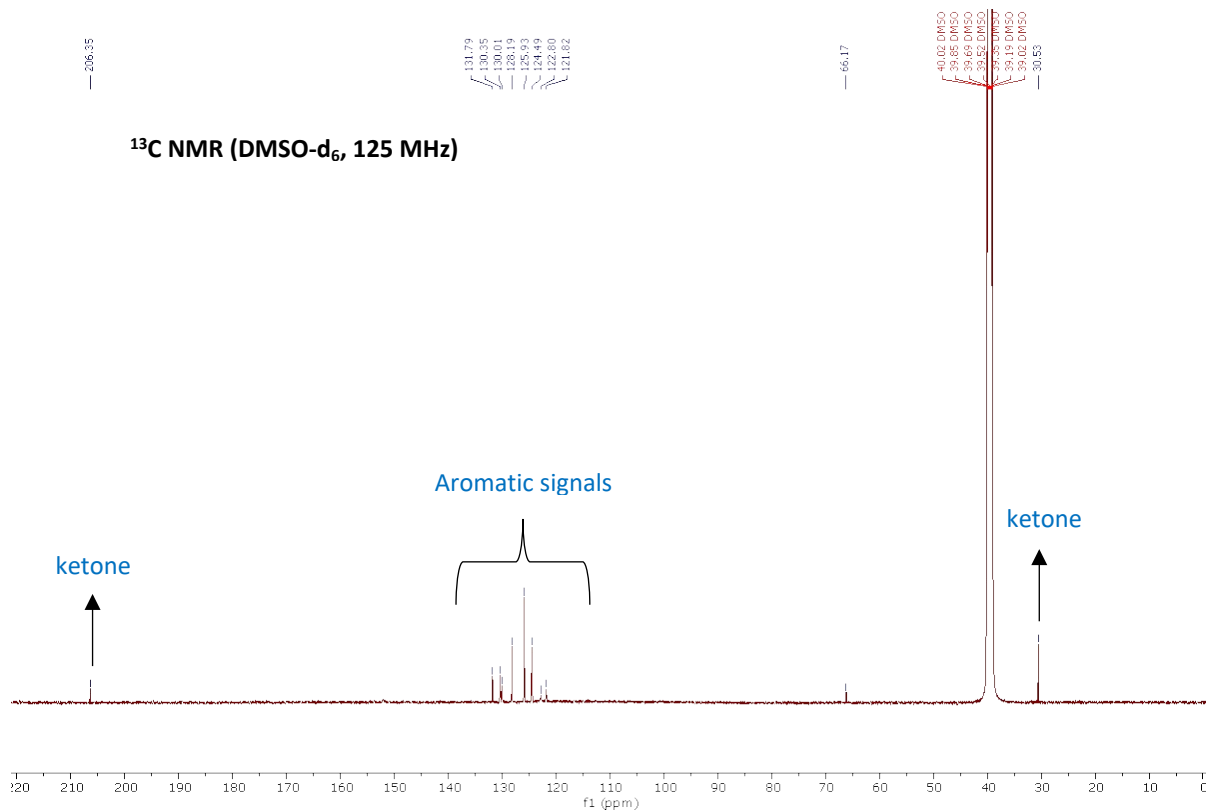
Fig. 2S-b. ^{13}C- NMR 125 MHz spectra of **1** in DMSO-d$_6$.

1.5. ESI-MS analysis for complex 1

A solution of 2.5 mg of **1** dissolved in 10 mL of MS-grade methanol was prepared. It was injected into the Waters SYNAPT XS ion mobility Q-TOF mass spectrometer in positive mode, being possible the identification of the fragment of [Cu$_2$(Phos$^-$)$_3$]$^+$, an adduct of the respective copper organometallic complex. On the other hand, a matrix of 15 mg of DCTB/mL in dichloromethane was prepared (DCTB = *trans*-2-[3-(4-*tert*-Butylphenyl)-2-methyl-2-propenylidene] malononitrile), allowing the identification of the fragment [Cu$_4$(Phos$^-$)$_7$]$^+$.

6

Table 2S. ESI-MS(+) of Complex **1**

Adduct	Formula	m/z calc.	m/z exp
$[Cu_2(Phos^-)_3]^+$	$C_{60}H_{36}O_{12}P_3{}^{63}Cu_2$	1167.0012	1167.0010
	$C_{60}H_{36}O_{12}P_3{}^{63}Cu^{65}Cu$	1168.9994	1169.0021
$[Cu_4(Phos^-)_7]^+$	$C_{140}H_{84}O_{28}P_7{}^{63}Cu_3{}^{65}Cu$	2683.0478	2683.0569
	$C_{140}H_{84}O_{28}P_7{}^{63}Cu_2{}^{65}Cu_2$	2685.0460	2685.0569
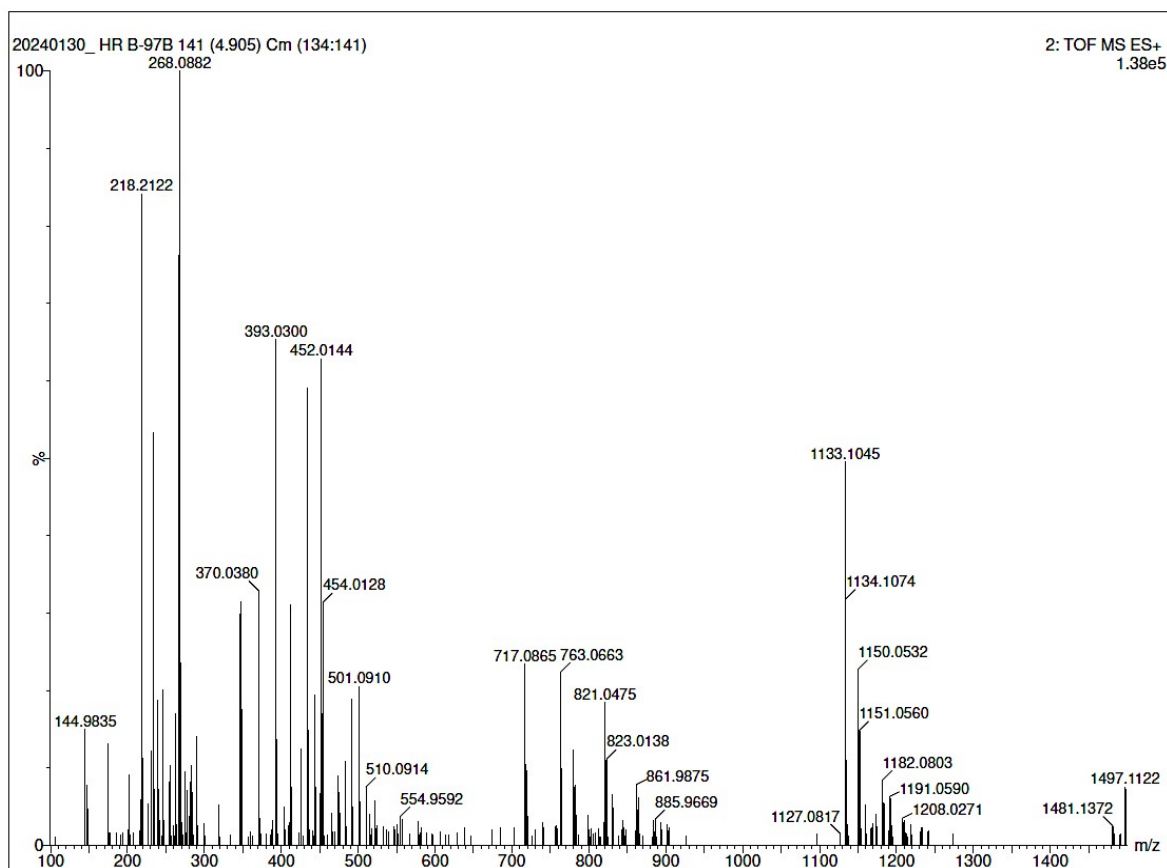
Fig. 3S-a. Experimental profile of the $[Cu_2(Phos^-)_3]^+$ cationic moiety.
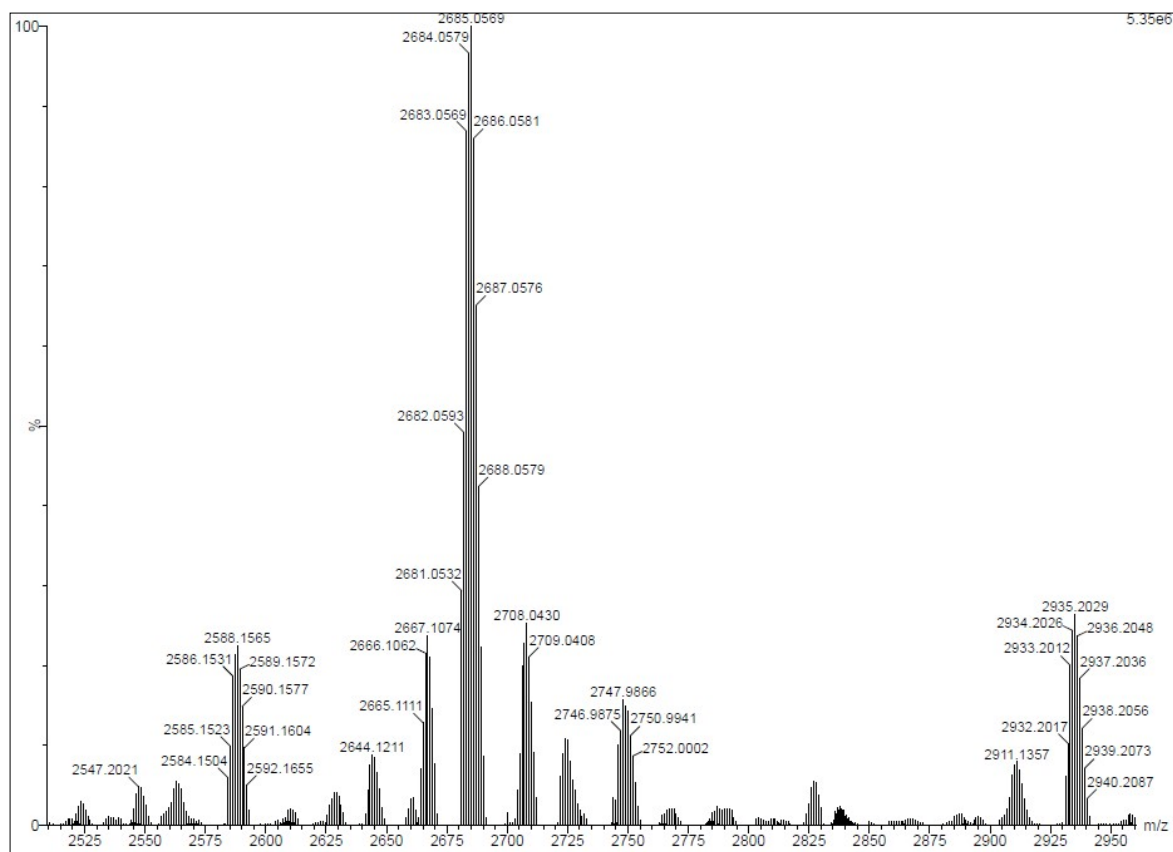
Fig. 3S-b. Experimental profile of the $[Cu_4(Phos^-)_7]^+$ cationic moiety.

2.0. X-Ray diffraction analysis for complex 1 $(C_3H_6O)_2$.

Data of complex **1** $(C_3H_6O)_2$, was obtained on a Rigaku Oxford Diffraction SuperNova (Cu) X-ray micro-focus source at room temperature, with Cu-K_α radiation (λ = 1.54184 Å). The data were indexed, integrated and scaled with the CrysAlisPro 1.171.43.104a (Rigaku Oxford Diffraction, 2023). The crystal structure was solved by direct methods using the SHELXT 2018/2 software,[1] with the Olex2 1.5 platform. The structure was refined by the full-matrix least-squares technique on F^2 with the SHELXL 2019/3 program.[2] All non-hydrogen atoms were refined anisotropically. The hydrogen atoms except those attached to the O-atoms of water molecules were introduced their idealized positions and refined in the isotropic approximation. Positional and anisotropic atomic displacement parameters were refined for all non-hydrogen atoms. Since we have used SQUEZZE procedure due to disorder of the dissolvent, the presence of the corresponding acceptor (OW2----H2WB) has probably been eliminated. The number of $(I_{obs}-I_{calc})/Sigma(W) > 10$ Outliers, was due to the presence of a small twin component that has not be considered in the data reduction. The asymmetric unit showing two independent neutral complexes in **1**·$(C_3H_6O)_2$: Cu1/Cu2 (I) and Cu3/Cu4 (II) is shown in **Fig. 4S**. The Flack parameter was refined to a value of -0.004(7) confirming the absolute structure.[3] Other experimental details are given in **Tables 3S** and **4S**. Mercury 2023.3.1 (CCDC, 2001-2013) program was used to visualize and study the hydrogen bonds and another interaction; whereas the Diamond 4.6.8 software was used to generate the structural drawings for this manuscript.[4] Crystallographic data for **1**·$(C_3H_6O)_2$ has been deposited in the Cambridge Crystallographic Data Center, with the CCDC number CCDC 2345065.

8
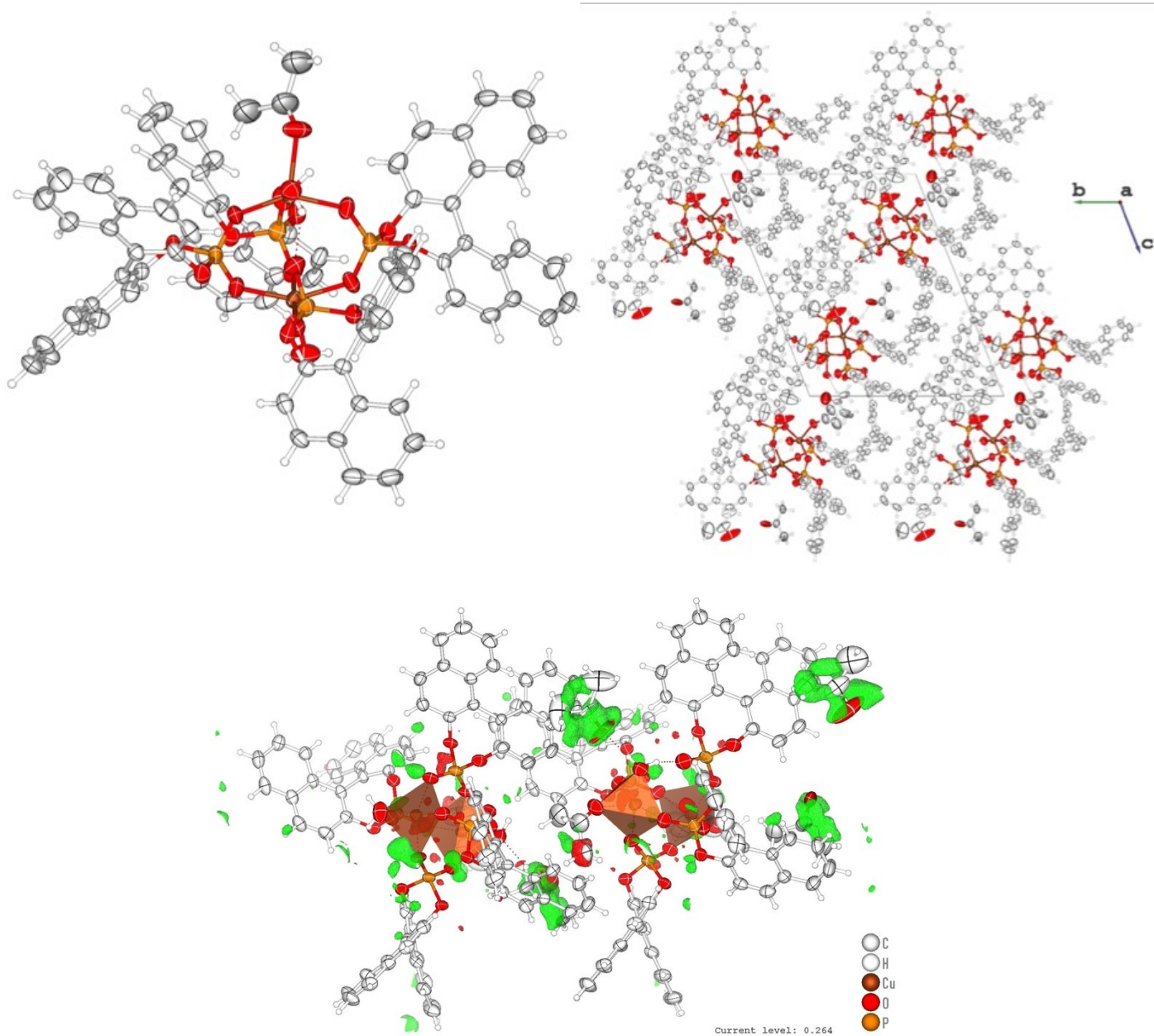
Fig. 4S. Structural drawing for complex **1** ($C_3H_6O)_2$: Cu1/Cu2 (I) and Cu3/Cu4 (II), ADP ellipsoids are shown at the 50% probability level; as well as residual density graph showing the difficulty of interpretation of the ketone molecules present.

Table 3S. Crystal data and structure refinement for complex **1·(C$_3$H$_6$O)$_2$**

Empirical formula	C$_{175}$H$_{132}$Cu$_4$O$_{40}$P$_8$
Formula weight	3376.72
Temperature/K	298(2)
Crystal system	triclinic
Space group	P1
Flack parameter	-0.004(7)
a/Å	11.2551(2)
b/Å	18.5480(3)
c/Å	22.4544(5)
α/°	107.266(2)
β/°	101.455(2)
γ/°	105.492(2)
Volume/Å^3	4112.34(15)
Z	1
ρ_{calcg}/cm^3	1.364
μ/mm^{-1}	1.967
F(000)	1738
Crystal size/mm^3	0.215 × 0.195 × 0.158
Radiation	Cu Kα (λ = 1.54184)
2Θ range for data collection/°	8.008 to 146.33
Index ranges	-13 ≤ h ≤ 13, -23 ≤ k ≤ 22, -25 ≤ l ≤ 27
Reflections collected	67768
Independent reflections	30348 [R$_{int}$ = 0.0326, R$_{sigma}$ = 0.0369]
Data/restraints/parameters	30348/197/2107
Goodness-of-fit on F^2	1.051
Final R indexes [I>=2σ (I)]	R$_1$= 0.0507, wR$_2$= 0.1526
Final R indexes [all data]	R$_1$= 0.0548, wR$_2$= 0.1580
Largest diff. peak/hole / e Å^{-3}	0.79/-0.71

Table 4S. Asymmetric unit of the two independent neutral complexes in **1**·$(C_3H_6O)_2$: Cu1/Cu2 (I) and Cu3/Cu4 (II)

Cu1/Cu2 (I) complex

Geometric of the **CuO_5 environment** (distance bonds in Å).

Cu1		Cu2	
Cu1 O43	2.001(4)	Cu2 O24	1.947(4)
Cu1 O33	1.956(4)	Cu2 O34	1.935(5)
Cu1 O13	1.945(5)	Cu2 O44	1.956(4)
Cu1 O23	1.988(4)	Cu2 O2W	1.942(5)
Cu1 O1W	2.141(5)	Cu2 O2A	2.222(5)

Geometric of the **CuO_5 environment** (angle bonds in °).

Cu1		Cu2	
O43 Cu1 O1W	97.0(3)	O24 Cu2 O44	146.7(2)
O33 Cu1 O43	87.8(2)	O24 Cu2 O2A	116.7(2)
O33 Cu1 O23	89.7(2)	O34 Cu2 O24	90.6(2)
O33 Cu1 O1W	89.1(2)	O34 Cu2 O44	94.7(2)
O13 Cu1 O43	91.3(2)	O34 Cu2 O2W	175.2(2)
O13 Cu1 O33	178.2(2)	O34 Cu2 O2A	91.3(3)
O13 Cu1 O23	90.4(2)	O44 Cu2 O2A	96.1(3)
O13 Cu1 O1W	92.5(2)	O2W Cu2 O24	86.4(2)
O23 Cu1 O43	149.1(2)	O2W Cu2 O44	89.8(2)
O23 Cu1 O1W	113.7(3)	O2W Cu2 O2A	86.7(2)

Addison parameter tau (τ_5) (angle bonds in °).[5]

Cu1 (τ = 0.49)		Cu2 (τ =0.48)	
O13 Cu1 O33	178.2(2)	O24 Cu2 O44	146.7(2)
O23 Cu1 O43	149.1(2)	O34 Cu2 O2W	175.2(2)

{$\tau = (\beta - \alpha)/60$, where $\beta - \alpha$ are the two largest ligand–metal–ligand angles of the coordination sphere}.

Geometric of the **PO_4 environment** (distance bonds in Å).

P1		P2		P3		P4	
P1 O11	1.607(4)	P2 O22	1.602(5)	P3 O32	1.605(4)	P4 O41	1.610(4)
P1 O12	1.612(4)	P2 O24	1.496(5)	P3 O33	1.477(5)	P4 O43	1.489(5)
P1 O13	1.485(5)	P2 O21	1.607(4)	P3 O31	1.598(5)	P4 O42	1.589(4)
P1 O14	1.467(5)	P2 O23	1.488(5)	P3 O34	1.488(5)	P4 O44	1.493(5)
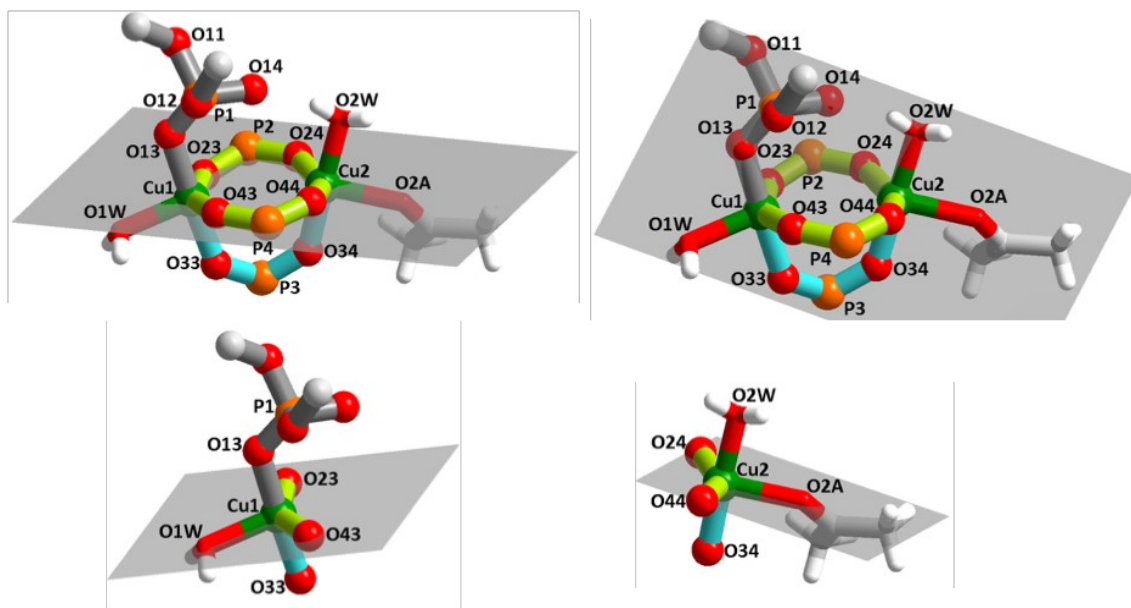
Fig. 5S-a. Planes of the eight- and five-members rings (P-O-Cu-O-P-O-Cu-O) and (Cu-O-P-O-Cu) and the respective equatorial CuO_3 planes. Visualized in the Cu1/Cu2 (I) complex.

Cu3/Cu4(I) complex

Geometric of the **CuO$_5$ environment** (distance bonds in Å).

Cu3		Cu4	
Cu3 O63	2.044(5)	Cu4 O64	1.941(5)
Cu3 O73	1.930(4)	Cu4 O74	1.951(5)
Cu3 O53	1.917(4)	Cu4 O84	1.939(5)
Cu3 O3A	2.170(6)	Cu4 O4A	2.239(5)
Cu3 O83	2.021(5)	Cu4 O4W	1.977(5)

Geometric of the **CuO$_5$ environment** (angle bonds in °).

Cu3		Cu4	
O63 Cu3 O3A	101.1(3)	O64 Cu4 O74	93.4(2)
O73 Cu3 O63	90.0(2)	O64 Cu4 O4A	95.8(2)
O73 Cu3 O3A	88.3(2)	O64 Cu4 O4W	90.8(2)
O73 Cu3 O83	90.0(2)	O74 Cu4 O4A	97.2(2)
O53 Cu3 O63	91.6(2)	O74 Cu4 O4W	175.7(2)
O53 Cu3 O73	175.3(2)	O84 Cu4 O64	158.9(2)
O53 Cu3 O3A	87.1(2)	O84 Cu4 O74	90.0(2)
O53 Cu3 O83	91.9(2)	O84 Cu4 O4A	104.5(2)
O83 Cu3 O63	136.0(2)	O84 Cu4 O4W	85.9(2)
O83 Cu3 O3A	122.9(2)	O4W Cu4 O4A	82.7(2)

Addison parameter tau (τ_5) (angle bonds in °).[5]

Cu3 (τ = 0.66)		Cu4 (τ =0.28)	
O53 Cu3 O73	175.3(2)	O74 Cu4 O4W	175.7(2)
O83 Cu3 O63	136.0(2)	O84 Cu4 O64	158.9(2)

{$\tau = (\beta - \alpha)/60$, where $\beta - \alpha$ are the two largest ligand–metal–ligand angles of the coordination sphere}.

Geometric of the **PO$_4$ environment** (distance bonds in Å).

P5		P6		P7		P8	
P5 O52	1.618(5)	P6 O61	1.603(4)	P7 O72	1.587(5)	P8 O81	1.613(5)
P5 O53	1.499(5)	P6 O62	1.607(5)	P7 O71	1.601(4)	P8 O82	1.600(5)
P5 O51	1.612(6)	P6 O64	1.498(5)	P7 O73	1.490(5)	P8 O84	1.489(5)
P5 O54	1.480(5)	P6 O63	1.480(5)	P7 O74	1.486(5)	P8 O83	1.482(5)
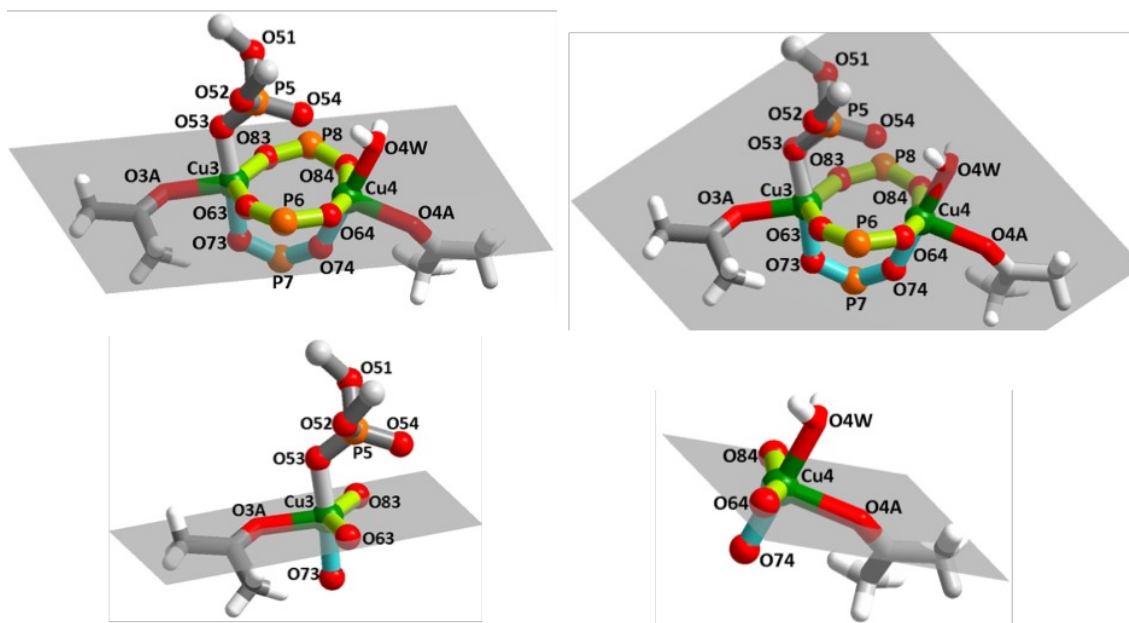
Fig. 5S-b. Planes of the eight- and five-members rings (P-O-Cu-O-P-O-Cu-O) and (Cu-O-P-O-Cu) and the respective equatorial CuO$_3$ planes. Visualized in the Cu3/Cu4 (II) complex.

References:

1   O. V. Dolomanov, L. J. Bourhis, R. J. Gildea, J. A. K. Howard and H. Puschmann, OLEX2: a complete structure solution, refinement and analysis program. *J. Appl. Crystallogr.* 2009, **42**, 339–341.

2   Sheldrick, G. M. Crystal structure refinement with SHELXL, *Acta Cryst.* 2015, **C71**, 3–8.

3   (a) Parsons, Flack and Wagner, *Acta Cryst.* 2013, **B69**, 249-259; (b) H.D. Flack and G. Bernardinelli, *Acta Cryst*. 1999, **A55**, 916-925; (c) D.J. Watkin and R.I. Cooper, *Chemistry,* 2020, 2(4), 796-804.

4   (a) Mercury 2023.3.1, Copyright © CCDC, 2001-2023; (b) K Brandenburg, DIAMOND-Crystal and Molecular Structure Visualization Version 4.6.8; Crystal Impact GbR: Bonn, Germany, 2022.

5   (a) A.W. Addison, T.N. Rao, J. Reedijk, J. van Rijn and G.C. Verschoor, *J. Chem. Soc., Dalton Trans*., 1984, 1349-1356; (b) M. Sharma, M. Sharma and N. Sharma, *Arabian Journal of Chemistry,* 2019, **12**, 5268–5277.

3. Thermal analysis for complex 1

Thermograms of TGA and DSC were obtained using a simultaneous TGA/DSC Discovery SDT 650 (TA Instruments). Measurements were performed with hermetically crimped Tzero aluminum crucibles (40 μL, 5 mg of **1**) under nitrogen atmosphere at a flow rate of 50 mL/min^{-1} from 26 to 500 C (at a heating rate of 10 C min $^{-1}$). The number of decomposition steps was identified using the derivative thermogravimetric curve (DTG).

(a)

(b)
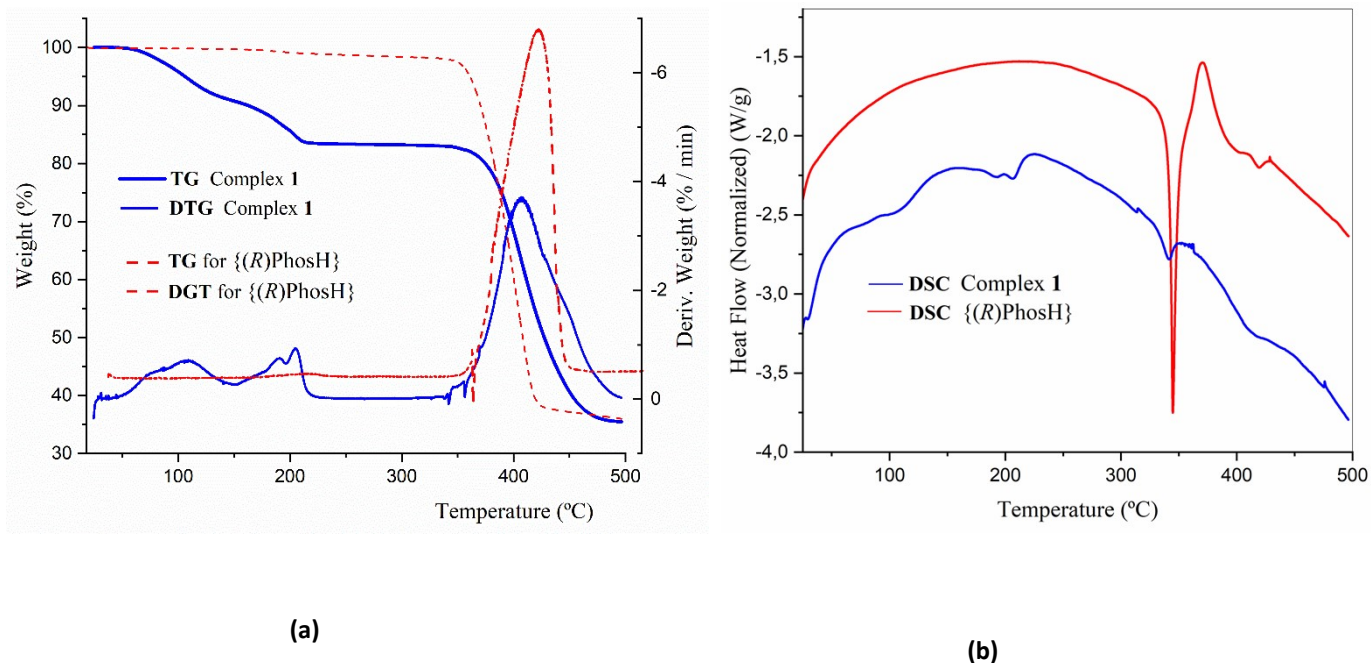
Fig. 6S. Comparative curves TG-DTG (a) and DSC (b) for **1** and compared with binaphthyl phosphoric acid {(*R*)-PhosH}.

4. Magnetic analysis for complex 1

4.1 Pd standard verification data prior to sample measurements.

Standard Pd verification using a 265.6 mg cylinder encapsulated with cotton in the SQUID Magnetometer- MPMS-3 equipment at 298 K, following a verification measurement sequence in DC mode. The measurement of the reference material shows an experimental deviation of less than 1% compared to the tabulated reference values.
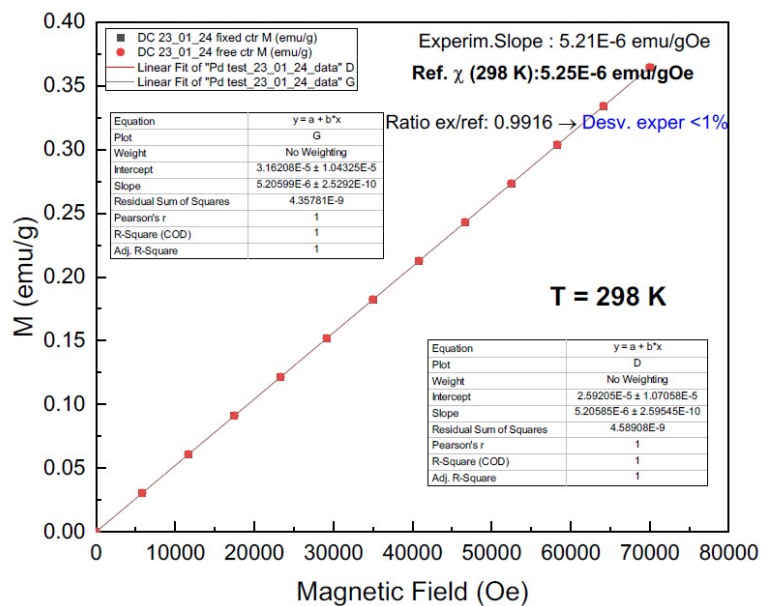
Fig. 7S-a. Verification in the SQUID Magneometer-MPMS-3 equipment.

4.2 Characterization.

A capsule is prepared with 23.3 mg of **1** and cotton, to compact and prevent the movement of the powdered sample when changing the temperature and/or the applied magnetic field. The measurement is carried out in a SQUID Magnetometer (Model MPMS-3, Quantum Design). The net magnetic signal is in the range of 10^{-3} to 10^{-4} emu for M-T measurements at 0.1T (1 kOe) applied magnetic field. In the measurements against a magnetic field, 0.16 emu is reached at 7 T (70 kOe) and 1.8 K. Considering the amount of sample measured, the magnetization values turn out to be appreciable. The magnetic signal shows an optimal magnitude with an extremely low noise level.
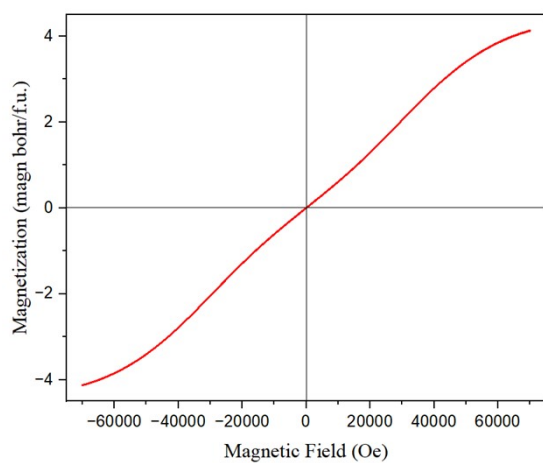
(a)
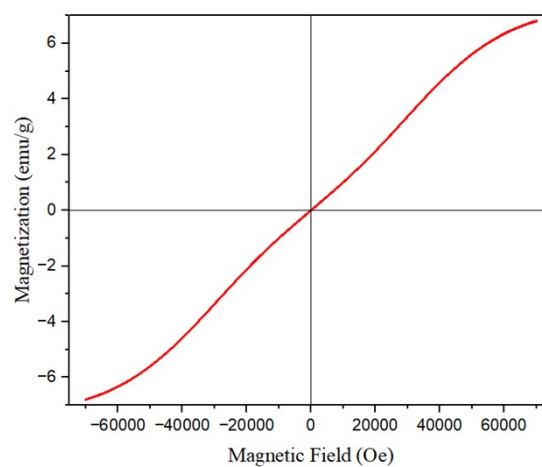
(b)

Fig. 7S-b. Magnetization measurements against magnetic field, up to 7 Tesla (70 kOe), of Cu-Complex sample at low temperature (1.8 K) in different units a) Magnetization (magn bohr/f.u.) vs. Magnetic Field (Oe) and b) Magnetization (emu/g) vs. Magnetic Field (Oe).
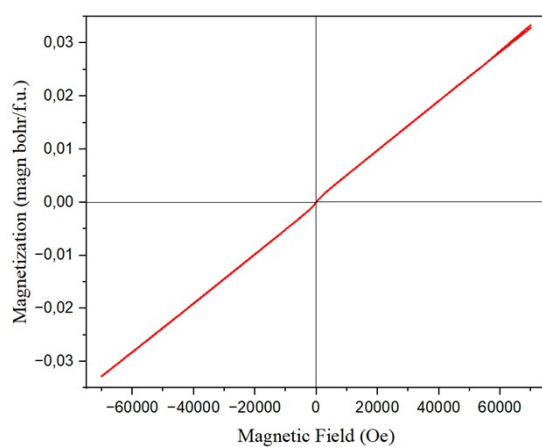
(a)
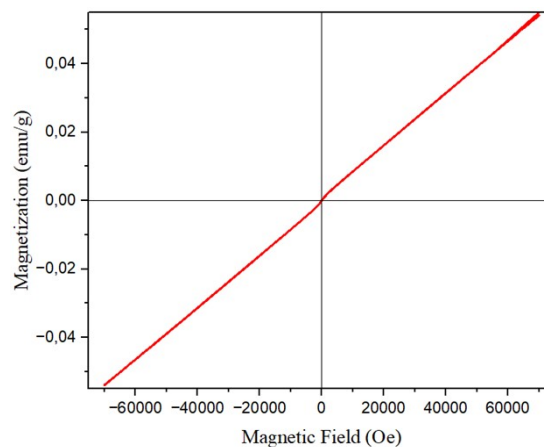
(b)

Fig. 7S-c. Magnetization measurements against magnetic field, up to 7 Tesla (70 kOe), of Cu-Complex sample at low temperature (300 K) in different units a) Magnetization (magn bohr/f.u.) vs. Magnetic Field (Oe) and b) Magnetization (emu/g) vs. Magnetic Field (Oe).

The linear fitting of the inverse of the magnetic susceptibility has been performed for both the ZFC and FC curves across various temperature ranges, with fittings at higher temperatures being more representative. From the range of values obtained, the error in the experimental value of the paramagnetic moment has been estimated.

Equation	y = a + b*x
Plot	1/X
Weight	No Weighting
Intercept	−15,19334 ± 0,3508
Slope	0,74039 ± 0,00228
Residual Sum of Squares	27,11391
Pearson's r	0,99961
R-Square (COD)	0,99922
Adj. R-Square	0,99921

(a)

Equation	y = a + b*x
Plot	1/X
Weight	No Weighting
Intercept	−13,38545 ± 0,27966
Slope	0,72726 ± 0,00183
Residual Sum of Squares	39,08228
Pearson's r	0,99965
R-Square (COD)	0,9993
Adj. R-Square	0,9993

(b)
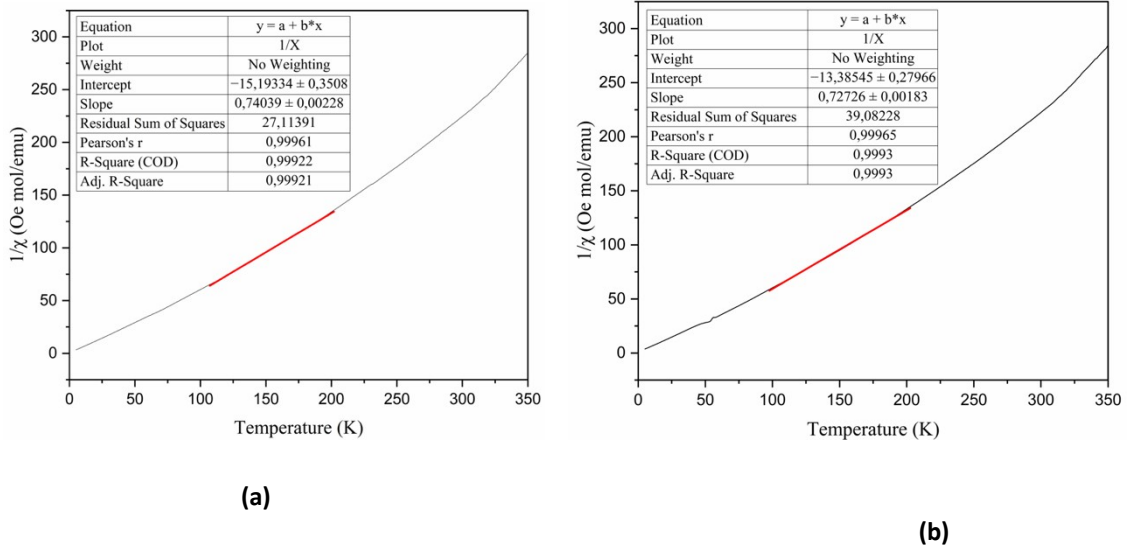
Fig. 7S-d: a) The ZFC curve of $1/\chi$ versus temperature and its linear fit and b) The FC curve of $1/\chi$ versus temperature and its linear fit.
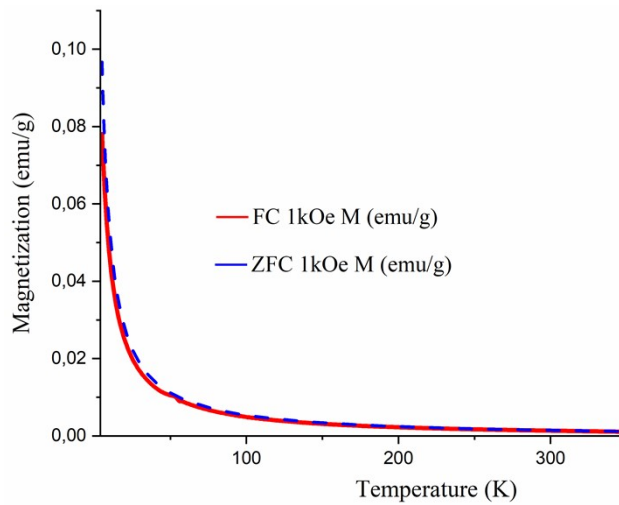
Fig. 8S. FC and ZFC curves.

5. Optical analysis for complex 1.

Diffuse reflectance spectra were made using a spectrophotometer equipped with an integrating sphere (Cary 5000). Emission and excitation spectra were measured using a photoluminescence spectrometer (Edinburgh Instrument FLS1000).
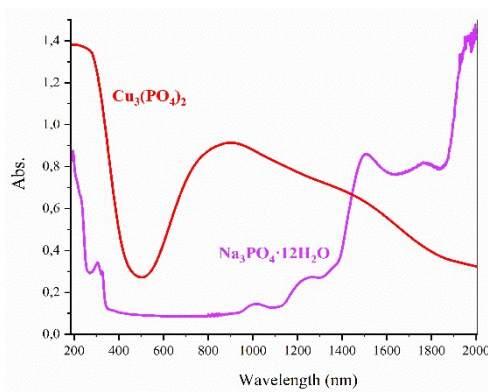
Fig. 9S: Diffuse reflectance spectra of the $Cu_3(PO_4)_2$ and $Na_3PO_4·12H2O$ matrices, as representative of the phosphate structures.